Received: 17 March 2021 | Accepted: 31 May 2021

DOI: 10.1111/1365-2664.13940

RESEARCH ARTICLE

Journal of Applied Ecology BRITISH ECOLOGICAL SOCIETY

Increased sediment deposition triggered by climate change impacts freshwater pearl mussel habitats and metapopulations

Damiano Baldan[1,2] | Jens Kiesel[3,4] | Christoph Hauer[5] | Sonja C. Jähnig[3,6] | Thomas Hein[1,2]

[1]Institute of Hydrobiology and Aquatic Ecosystem Management, University of Natural Resources and Life Sciences (BOKU), Vienna, Austria; [2]Wassercluster Lunz - Biologische Station, Lunz am See, Austria; [3]Department of Ecosystem Research, Leibniz Institute of Freshwater Ecology and Inland Fisheries, Berlin, Germany; [4]Institute for Natural Resource Conservation, Department of Hydrology and Water Resources Management, Christian-Albrechts-University Kiel, Kiel, Germany; [5]Christian Doppler Laboratory for Sediment Research and Management, Institute of Hydraulic Engineering and River Research, University of Natural Resources and Life Sciences (BOKU), Vienna, Austria and [6]Geography Department, Humboldt-Universität zu Berlin, Berlin, Germany

Correspondence
Damiano Baldan
Email: damiano.baldan@wcl.ac.at

Thomas Hein
Email: thomas.hein@boku.ac.at

Funding information
CEEPUS network EcoManAqua, Grant/Award Number: CIII-AT-1101-03-1819; GLANCE, Grant/Award Number: 01LN1320A; Niederösterreiche Forschungs- und Bildungsgesellschaft, Grant/Award Number: SC17-002; Doctoral School "Human River Systems in the 21st Century (HR21)" of the University of Natural Resources and Life Sciences (BOKU), Vienna; EU-INTERREG FRAMWAT, Grant/Award Number: CE983; Leibniz Competition for the project "Freshwater Megafauna Futures"; CRC RESIST, Grant/Award Number: 426547801

Handling Editor: Melinda Coleman

Abstract

1. The freshwater pearl mussel *Margaritifera margaritifera* is a benthic organism sensitive to hydrological regime alterations and habitat degradation driven by excessive fine bed material deposit (FBMD). Both issues are potentially exacerbated by climate change. Understanding how climate change affects future mussel habitats and the dispersal among them (dependent on the brown trout as fish host) can support the planning of effective conservation actions.
2. To project the impacts of climate change on the mussel, a semi-mechanistic modelling cascade was implemented for the Aist catchment in Austria (630 km^2), including a hydrological model, a hydraulic model, Random Forest Models for FBMD accumulation risk and Species Distribution Models. Two climate change models (RCPs 4.5 and 8.5) for two future horizons (2060 and 2090) were considered. A graph-based assessment of the structural connectivity was used to measure the probability of successful dispersal.
3. Results show a reduction of peak discharge that cascades into a widespread reduction in shear stresses during high flow. The mussel's habitats, defined by hydraulics (i.e. patches with low shear stresses during high flow), are predicted to be stable over the simulated scenarios.
4. The pressure of FBMDs over the delineated habitat patches is predicted to increase in the future due to the reduced stream transport capacity, reducing up to 25% of the available patches in 2090 for RCP 8.5. Consequently, the mussel's dispersal probability decreases to 44.3%–75.6% of the maximum theoretical value, with the highest drops for short dispersal distances, impacting metapopulation dynamics.
5. *Synthesis and applications*. The widespread issue of fine sediment deposition in the streambed will be exacerbated for those catchments where climate change

reduces the stream transport capacity. The impacts on the freshwater pearl mussel include habitat loss due to the formation of a new unsuitable substrate, and a decrease in the potential dispersal among the residual habitats. Thus, conservation plans that aim to protect the mussel in the future should focus on the mitigation of fine bed material deposits, prioritizing those subreaches that offer the highest potential for preserving connectivity among suitable habitats.

KEYWORDS

climate change, ecohydrological modelling cascade, fine sediments deposition, freshwater biodiversity conservation, freshwater habitat modelling, freshwater pearl mussel, metapopulation connectivity

1 | INTRODUCTION

Climate change is a major driver of alterations in river ecosystems, affecting hydrological regimes, sediment dynamics (Hagemann et al., 2013), and interacting with additional stressors such as habitat loss. The resulting impacts on freshwater biota include habitat range shifts and fragmentation (Fuller et al., 2015). To effectively halt freshwater biodiversity losses, proactive conservation plans that account for current and future species distributions are needed (Bush et al., 2014). However, two aspects complicate climate change-resilient conservation planning in freshwater systems.

The first aspect is related to incorporating causal relationships when projecting the impacts of climate change on biota. Correlative models can support freshwater conservation planning by assessing present and future species distributions (Bush & Hoskins, 2017), but extrapolations can be highly uncertain (Yates et al., 2018). Ecohydrological modelling cascades are sequences of interlinked models covering different spatial scales (catchment, reach, sites) and domains (hydrology, hydraulics, biota distribution) that support the development of causal relationships for biota distribution and thus improve the reliability of future extrapolations (Jähnig et al., 2012). Due to the increased complexity involving interdisciplinary integration and significant modelling effort (Kail et al., 2015), widespread use of ecohydrological modelling cascades is lacking. However, the development of causal relationships can be beneficial to support conservation planning for highly relevant organisms.

The second aspect involves the difficulty of modelling habitat preferences for species with complex life cycles, especially when the dispersal relies on other organisms (Inoue et al., 2017). For instance, freshwater mussels are benthic organisms with a life cycle that includes an obligate parasitic phase on a host fish, where the larvae (glochidia) develop into juveniles (Modesto et al., 2018). Juveniles bury themselves in the hyporheic zone before emerging as adults (Geist, 2010). As disturbances can impair every life stage, identifying bottlenecks is essential for developing successful conservation plans (Geist, 2010).

This study focuses on the freshwater pearl mussel *Margaritifera margaritifera* (L., 1758), a cold water adapted mussel with a narrow habitat niche (Varandas et al., 2013). The mussel's 9-month parasitic phase occurs exclusively on the brown trout and the Atlantic salmon, followed by a 5-year juvenile and long-lived adult phase (up to >100 years). The mussel's distribution is highly clustered in subreaches, where the hydrodynamic conditions do not lead to significant substrate mobilization during high flows (Figure S1 in Supporting Information; Morales et al., 2006; Sousa et al., 2015). The mussel's metapopulations rely on glochidia dispersal and juvenile survival to colonize new suitable patches (Geist, 2010).

The freshwater pearl mussel is classified as 'Endangered' globally and 'Critically Endangered' in Europe by the International Union for the Conservation of Nature Red List of Threatened Species (IUCN, 2021). In Europe, it has been the target of standardized monitoring programs (Boon et al., 2019) and several conservation actions, given its importance as an 'umbrella' species (Geist, 2010). The freshwater pearl mussel is sensitive to changes in the hydrological regime, including intense floods (Sousa et al., 2012), prolonged droughts (Sousa et al., 2018), alteration due to small hydropower plants (Sousa et al., 2020) and climate change, including water temperature changes (Bolotov et al., 2018; Santos et al., 2015). Climate change can additionally lead to increased soil erosion, affecting the sediment balance in streams (Hauer, 2015). Fine sediment transport and deposition (as fine bed material deposits, FBMDs) was identified as a major driver for population impairment, as it affects both substrate quality and stability (Denic & Geist, 2015; Geist & Auerswald, 2007; Hoess & Geist, 2020; Österling et al., 2010). Thus, conservation planning for the freshwater pearl mussel needs to consider climate change effects.

Given the knowledge gaps and challenges for climate change assessments outlined above, the aims of this study were as follows: (a) to use an ecohydrological modelling cascade to project the impacts of climate change on catchment-scale hydrology, sediment generation, reach-scale hydraulics, mesohabitat scale FBMD accumulations and freshwater pearl mussel habitat; and (b) to assess the impacts of climate change on the mussel, both direct (range shift) and indirect (increased FBMD deposition and limitation to organism dispersal).

2 | MATERIALS AND METHODS

2.1 | The Aist catchment

The Aist catchment (630 km^2, Figure 1) has a temperate climate with an average annual temperature of 7.1°C and average annual precipitation of 835 mm (HDLO, 2017). Rivers in the Aist catchment (Feldaist, Waldaist and Aist river) have a 'plane bed' morphology with cobble as the dominating substrate (Hauer, 2015), and suffer from accumulations of coarse sand to fine gravel (modal diameters: 1–10 mm) originating from the weathering of the geological bedrock. Given the difference with the homogeneous grain sizes compared to the substrate at reference sites and the increased mobility, such accumulations can be classified as FBMDs. The impacts of climate change already documented in this and surrounding catchment include increases in local heavy rainfall events leading to increased soil erosion, decreasing discharges in summer months and reduction of habitats for salmonid fish species (Hauer, 2015; Hauer et al., 2013, 2015).

2.2 | The ecohydrological modelling cascade

The ecohydrological modelling cascade used to project the climate change effects includes the following interlinked models (Figure S2; Table 1; Baldan, Mehdi, et al., 2020; Baldan, Piniewski, et al., 2020):

1. The hydrological Soil and Water Assessment Tool (SWAT 2012 v670) to simulate discharge and sediment generation and transport at the catchment scale;
2. The hydrodynamic numerical 1D-model Hydraulic Engineering Centre – River Analysis System (HEC-RAS v5.0.5) to simulate hydraulics at the river reach scale;
3. An ensemble of Random Forests (RFs, R package 'caret') to classify the FBMD risk at the mesohabitat scale;
4. Species Distribution Models (SDMs, R package 'biomod2') to predict the adult freshwater pearl mussel occurrence at the mesohabitat scale;
5. a connectivity assessment (CONEFOR v2.6) to estimate the probability of successful colonization given the spatial arrangement of suitable habitat patches.

SWAT uses climatic, land use and soil data for semi-distributed, long-term hydrological simulations on a daily time step. Climatic inputs to SWAT are daily precipitation and temperature data, which can be either measured time series or the outputs of climate models. The latter were used here and allowed for climate change simulations. The hydrological outputs were processed to derive (a) relevant indicators of hydrological alterations (IHAs; Olden & Poff, 2003) and (b) the 20th, 50th and 90th flow percentiles (low, mid and high flow) used as inputs of steady-state flow profiles in HEC-RAS. HEC-RAS models reach hydraulics (e.g. cross-sectional averaged flow velocity, water depth and shear stress; Table 2).

SWAT was calibrated and validated for 2002–2016 (refer to Baldan, Piniewski, et al., 2020 for further details on calibration and performance). As measured by the Kling-Gupta efficiency (KGE, Gupta et al., 2009), SWAT performed well for both calibration (KGE = 0.70 ± 0.12 for flow and 0.67 ± 0.21 for sediments, standard deviation represents variability across five flow and sediment gauges) and validation (KGE = 0.78 ± 0.10 for flow and

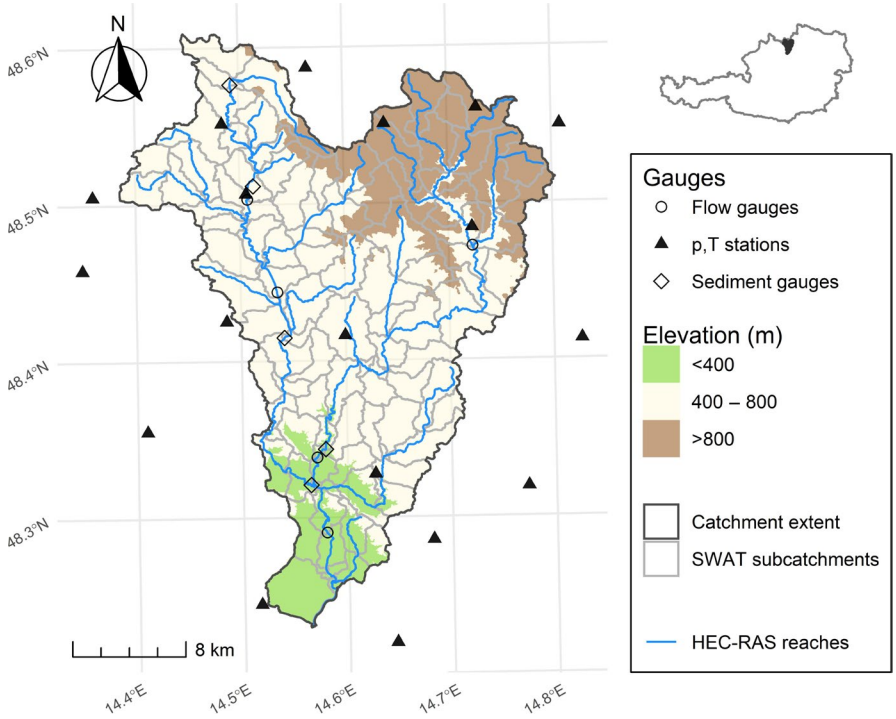

FIGURE 1 Map of the Aist catchment showing the position of the precipitation (*p*) and temperature (*T*) stations used to correct bias across all climate models, the position of discharge and sediment gauges used to calibrate SWAT and its subcatchments and the reaches modelled with HEC-RAS

TABLE 1 Models implemented in the modelling cascade

Model	Spatial coverage	Spatial resolution	Spatial scale
SWAT	Aist catchment, 630 km^2	5.5 ± 5 km^2	Catchment
HEC-RAS	Aist river, 280 km, 11,000 cross sections	25 m	Reach
Random Forest ensemble, SDMs	Aist river, 5,700 raster cells	50 × 50 m	Mesohabitat
CONEFOR	Aist river system, subreaches	300–2,700 m	Habitat patches

TABLE 2 List of SWAT and HEC-RAS outputs used as predictors in RFs and SDMs

Category	Output/predictor	Description	Units	Source	Used in
Sediment	Peak upstream input[a]	90th percentile of the SWAT sediment yield normalized by the drainage density and cumulated for upstream subcatchments	t km^{-1} $month^{-1}$	SWAT	RFs
Hydrology	Duration high flow[a]	Annual maxima of 7-day means of daily discharge	m^3/day	SWAT	RFs
Hydrology	Frequency high flow[a]	Mean yearly number of events where the flow exceeds two times the median discharge	—	SWAT	RFs
Hydrology	Magnitude high flows[a]	Mean of the 10th flow divided by the median daily flow across all years		SWAT	RFs
Hydrology	Magnitude low flows[a]	Median of the lowest annual daily flows divided by median annual daily flows averaged across all years	—	SWAT	RFs
Hydrology	High flow discharge[a]	Flow percentile that exceeds 90% of the recorded discharge	m^3/s	SWAT	HEC-RAS
Hydrology	Mean flow discharge[a]	Flow percentile that exceeds 50% of the recorded discharge	m^3/s	SWAT	HEC-RAS
Hydrology	Low flow discharge[a]	Flow percentile that exceeds 20% of the recorded discharge	m^3/s	SWAT	HEC-RAS
Hydraulics	Low flow velocity	Cross-sectional average of flow velocity calculated with the 10th discharge percentile	m/s	HEC-RAS	RFs, SDMs
Hydraulics	High flow shear stress	Cross-sectional average of shear stresses, calculated with the 90th discharge percentile	Pa	HEC-RAS	RFs, SDMs
Hydraulics	Mean flow water depth	Cross-sectional average of flow depth; for median discharge	m	HEC-RAS	RFs

[a]Sediment and hydrology predictors were used in the climatic model selection.

0.63 ± 0.17 for sediment). Water surface elevation for HEC-RAS calibration was measured at three representative reaches, with 10 cross sections each (250 m sections) during low flow conditions between September and November 2014. The difference between the measured and modelled water surface elevation was always smaller than 3 cm (e.g. <10% of the water depth during low flow, considered acceptable according to Bolla Pittaluga et al., 2014). As field measurements of water surface elevation were not possible during high flow conditions, the calibrated roughness values from a flood hazard analysis study for the Aist system were applied (Hauer et al., 2015). SWAT and HEC-RAS outputs from runs covering the period 2002–2013 (hereafter historical) were rasterized along the channel centrelines to generate the inputs (hereafter predictors, Table 2; resolution: 50 m × 50 m; n = 5,700 raster cells) used for the development of predictive relationships for FBMDs with the RFs and mussel's habitat with the SDMs.

Field data classifying the FBMD occurrence on a five-level risk scale (Figure S3; Table 3; Hauer et al., 2015) were used to train the RF ensemble based on the predictors developed in the previous steps (Table 2), yielding an acceptable performance (Accuracy = 0.72 ± 0.02; Kappa = 0.61 ± 0.02; Allouche et al., 2006). The RFs associate a high FBMD occurrence risk with low values of high flow shear stresses (i.e. transport-limited sites), while sites with low FBMD risk have low upstream peak sediment loads (i.e. supply-limited sites; Table 3; Baldan, Mehdi, et al., 2020).

2.3 | Appropriate climate model selection

A combination of a global circulation model (GCM) and a regional climate model (RCM) for the two representative concentration pathways (RCPs) 4.5 and 8.5 was selected from the EURO-CORDEX repository (complete list in Figure S3). First, daily precipitation (1984–2016) and temperature (1999–2016) data from 13 weather stations (Figure 1) were used to bias-adjust all EURO-CORDEX models using distribution mapping (Switanek et al., 2017) implemented

TABLE 3 Descriptions and controlling factors for fine bed material deposit risk classes. The three most relevant factors identified in the RFs are listed (in decreasing importance order). The dependence linking the risk class likelihood each predictor is in parenthesis: *M* = maximum, m = minimum, upwards arrow (↗) = monotonous response with a positive slope; downwards arrow (↘) = monotonous response with a negative slope

FBMD risk class	Description	Influence of predictors
0	No alteration in the natural substrate	High flow shear stress (↗), peak sediment input (M), low flow velocity (M)
1	Little disturbance	High flow shear stress (↗), low flow velocity (M), high flow water depth (M)
2	Some habitat changes but main morphological features are kept	High flow shear stress (↗), high flow water depth (M), peak upstream input (M)
3	Mesohabitat is fully covered	High flow shear stress (↗), low flow velocity (↗), high flow water depth (↘)
4	Mesohabitat is fully covered, the substrate is mobile during low flow conditions	High flow shear stress (↘), low flow velocity (m), high flow water depth (↘)

in the software CMhyd (Rathjens et al., 2016). Second, SWAT was executed for 2002–2016 using both the observed and the climate-model-derived precipitation and temperature data (hindcasted predictions). Finally, modelled and hindcasted hydrological predictions (Table 2) were compared based on the Euclidean distance (Kiesel et al., 2019). The climate model minimizing the Euclidean distance was used for the subsequent analysis (GCM: ICHEC-EC-EARTH; RCM: KNMI-RACMO22E, Figure S4). The selection is supported by an independent analysis carried out in the Danube catchment, which showed that the dataset derived from this model best predicts the already observed climate change impacts on streamflow (Kiesel et al., 2020).

2.4 | Climate change scenarios' definition and propagation

While the predictive relationships developed in the calibrations of the models (RFs; SDMs) are valid for the historical, 12-year-long period (2002–2013), a much larger period is needed to capture the long-term climatic trend and exclude natural variability as a possible impact factor. Thus, 36-year-long periods (time horizon) were used to extract daily precipitation and temperature data from the selected climate models. Time horizons studied included 1987–2022 (hereafter baseline), 2027–2062 (2060) and 2057–2092 (2090). In this study, the term 'scenario' denotes a unique combination of a time horizon and an RCP.

For each 36-year-long scenario, three consecutive, 12-year-long SWAT runs were performed with the bias-corrected precipitation and temperature scenario data. Hydrologic outputs (Table 2) were averaged among the three runs for each scenario. The averaging across the three 12-year-long periods is tolerable since the coefficient of variation across the SWAT subcatchments is small (Figure S5). Thus, predictive relationships developed for the historical period could still be used for scenarios with different simulation lengths. Averaged hydrologic outputs were passed along the cascade to hydraulics, RFs and SDMs for all the different scenarios.

For baseline versus scenario comparisons, SWAT and HEC-RAS predictors used in the following steps were rescaled with a delta change approach to account for nonlinearities in the responses (Figure S6). The rescaling allows to perform predictions for smaller deviations from the training dataset and can benefit correlative models (Yates et al., 2018). The relative change in each predictor P_i value in each raster cell for each scenario *sc* compared to the baseline scenario *base* was calculated, and a new scaled predictor $\widehat{P_{i,\mathrm{sc}}}$ was computed by multiplying this delta change with the historical predictor value $P_{i,\mathrm{hist}}$:

$$\widehat{P_{i,\mathrm{sc}}} = P_{i,\mathrm{hist}}\left(1 + \left(P_{i,\mathrm{sc}} - P_{i,\mathrm{base}}\right)/P_{i,\mathrm{base}}\right). \quad (1)$$

This method ensures that baseline predictors overlap with historical predictors.

2.5 | Habitat niche model for adult freshwater pearl mussels

Species Distribution Models (SDMs, R package BIOMOD2, Thuiller et al., 2009) were used to assess the potential freshwater pearl mussel distribution. The models were fitted to 69 presence/absence data points for the Aist catchment (Baldan, Piniewski, et al., 2020). Different algorithms were used, including a GLM, a generalized additive model (GAM), a generalized boosting model (GBM), a maximum entropy model (MaxEnt) and a random forest (RF) model. Each algorithm used a high number of pseudo-absences (500) and 10-fold cross-validation, following Barbet-Massin et al. (2012), for

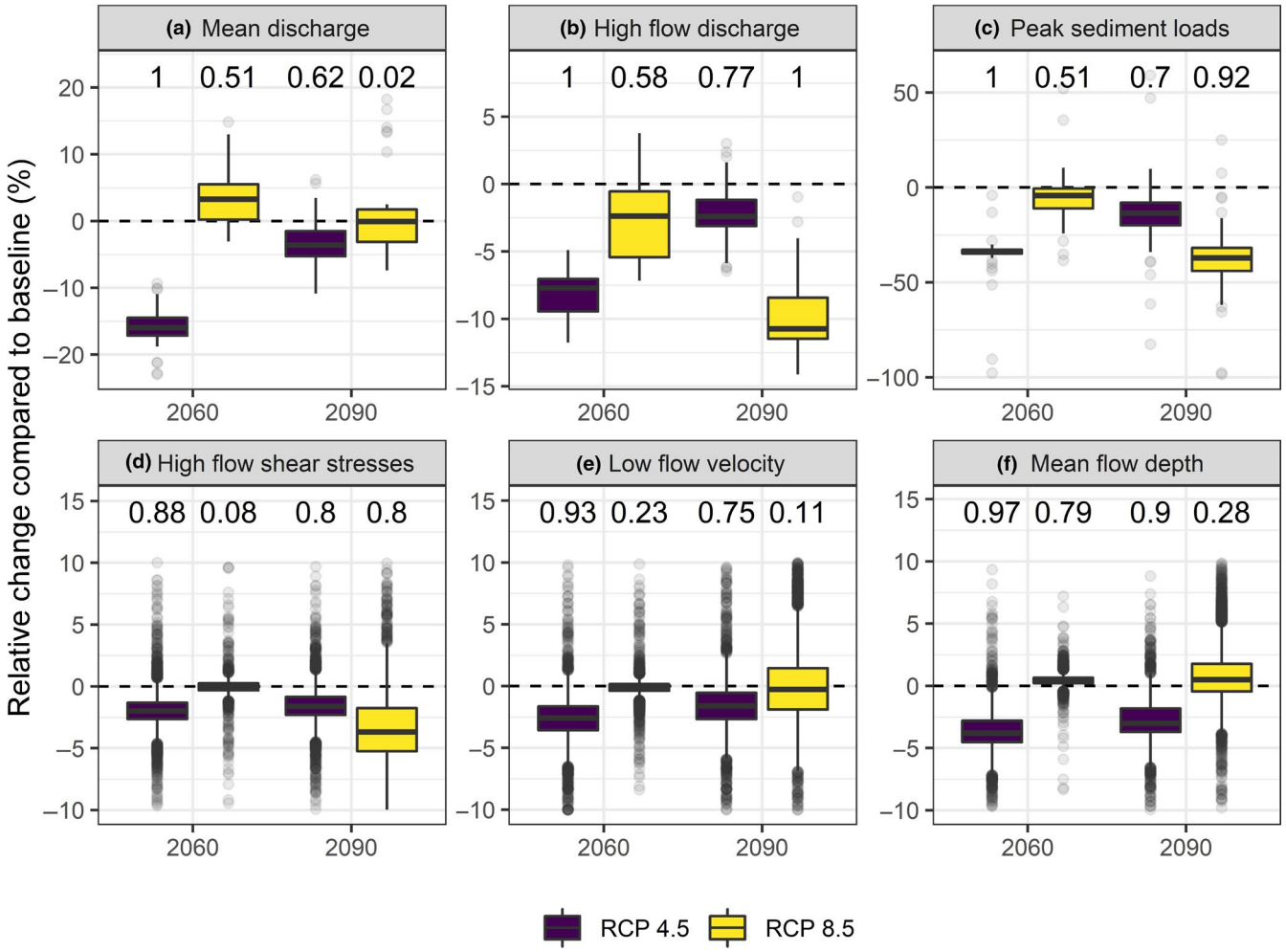

FIGURE 2 Impact of climate change on the most important predictors obtained from SWAT and HEC-RAS model results. Boxplots represent variation across SWAT subcatchments (subplots a–c, $n = 103$) or across river network raster cells (subplots d–f, $n = 5,700$). The annotation on top of each boxplot represents the DC index. Refer to Table 2 for the definition of the predictors

a total of 50 fitted models. Because of the small size and spatial coverage of the dataset used to train the SDMs, only hydraulic predictors (shear stress during high flow and average flow velocity, Figure 2) were used to fit the models (Jähnig et al., 2012). Land use-related predictors were not included, given the unavailability of future land use trajectories. The ensemble model was obtained from the weighted average of the single algorithm models (Thuiller et al., 2009) by multiplying the area under the receiving operating characteristic curve (AUC) scores with a decay of 1.6 (default value). The ensemble habitat model has a good discriminatory capacity (AUC = 0.81; Allouche et al., 2006). The output of the ensemble model is the spatial distribution of the Habitat Suitability Index (HSI, range 0 to 1). Suitable and unsuitable habitats were discriminated against by setting an HSI threshold (0.5) that balances omission and commission errors. Changes in the HSI values between baseline and scenario simulations were assessed with a paired *t*-test.

The partial dependence plots show that the freshwater pearl mussel prefers sites with low shear stress during high flows (<25 Pa) and avoids sites with low average flow velocity (Figure S7). Based on the HSI output, habitat patches were delineated as suitable with contiguous suitable habitats (raster cells) of a minimum length of 300 m (i.e. a minimum area of 1,500 m^2; Vaughn, 2012).

2.6 | Potential harm to habitat due to FBMDs

When a site gets affected by FBMDs, the likelihood of survival for the mussel decreases for both juveniles (Denic & Geist, 2015; Geist & Auerswald, 2007) and adults (Hauer, 2015). The Accumulation Risk Index (ARI) was calculated to assess the impacts of FBMDs for each delineated habitat patch. For each patch, ARI was defined as the arithmetic mean between the average and the highest modelled FBMD risk class (Table 3; Baldan, Piniewski, et al., 2020). ARI ranges between 0 and 4, with low values for unimpaired patches and high values for patches affected by high-risk classes of FBMDs. The harm of FBMDs to the mussel's habitats was assessed as the decrease in the total number and extent of habitat patches when habitat patches

having high ARI are excluded. A conservative threshold that maximizes the habitat loss was used (ARI = 3.4, Figure S8).

2.7 | Assessment of the potential mussel dispersal

A graph-theory analysis was used to estimate the impact of FBMDs on the inter-patch dispersal potential (i.e. structural connectivity). Based on the spatial arrangement of the delineated habitat patches, a graph was created, where nodes are the habitat patches and links are the potential connections between patches separated by non-suitable habitats along the river network. The probability of dispersal between two suitable habitat patches was modelled with a negative exponential probability density function parametrized with the average dispersal distance, corresponding to the movement distance of the brown trout encysted by glochidia (the brown trout is the only fish host in the Aist catchment). Three different dispersal distances were tested, representing a lower (200 m), a median (1,000 m) and an upper estimate (5,000 m; Young et al., 2010).

The PCinter index was used to measure the structural connectivity of the delineated graph (Saura & Rubio, 2010; Ward et al., 2020) when habitat patches are assigned equal weights:

$$\mathrm{PCinter} = \frac{\sum_{i=1}^{n} \sum_{j=1, i \neq j}^{n} p_{ij}^{*}}{n^2}, \quad (2)$$

where p_{ij}^{*} is the maximum dispersal probability among all the possible links between patches i and j and n is the total number of patches. The PCinter index measures the network-averaged probability of a successful dispersal/recolonization event.

Following Ward et al. (2020), for each scenario, the index PCinter was recalculated by setting the probabilities $p_{ij}^{*} = 0$ when either patch i or j are affected by FBMDs (namely $\mathrm{PCinter}_{sc}$). Then, the residual PCinter fraction (namely $\mathrm{PCinter}_{res}$) was calculated as:

$$\mathrm{PCinter}_{res} = \frac{\mathrm{PCinter}_{sc}}{\mathrm{PCinter}_{all}} \times 100, \quad (3)$$

where $\mathrm{PCinter}_{all}$ is the PCinter calculated for the unimpaired networks. Dispersal barriers were not included, given the uncertainty in the passability estimation (Buddendorf et al., 2019). However, our results are robust concerning this simplification, as only relative changes in connectivity were assessed.

Confidence intervals (95%) of the PCinter drop estimates were assessed via bootstrapping, that is by randomly removing habitat patches from the analysis to generate subsets of the original graph and repeating the analysis for each subset (500 repetitions). The consistency of the average bootstrapped PCinter drops was assessed with the pseudostatistic 'direction of the change' index (DC), a non-parametric measure of the fraction of an index distribution exceeding a threshold (Figure S9). The DC ranges between 0 and 1, with DC = 1 when all the replicate PCinter drops are positive or negative (clear direction of the change) and DC = 0 when the distribution of PCinter drops is centred on 0 (unclear direction of the change).

3 | RESULTS

3.1 | Impacts of climate change on hydrology and hydraulics

The bias-corrected climate data show changes in precipitation patterns, including a slight decrease in precipitation in 2060 for RCP 4.5 (Figure S10), coupled with increases in air temperature in the future that peak in 2090 for RCP 8.5 (Figure S11). Hydrological impacts of climate change in the Aist catchment include an increase in evapotranspiration, a reduction in snowmelt contribution to discharge (Figure S12) and a reduction in water yield (Figure S13), resulting in a reduction of mean and high flow discharge in 2060 for RCP 4.5 (−16% and −8% relative average change compared to baseline respectively; Figure 2a,b) and a reduction of high flow discharge in 2090 for RCP 8.5 (−10%, Figure 2b). Additionally, the maximum water yield occurs later for RCP 8.5 (Figure S13). The high flow shear stresses are on average reduced up to −3.6% in 2090 for RCP 8.5 (Figure 2d), and low flow velocity is on average reduced up to −2.9% in 2060 for RCP 4.5. Peak sediment loads are reduced by 33% in 2060 for RCP 4.5 and 37% in 2090 for RCP 8.5 (Figure 2f).

3.2 | Impact of climate change on the habitats of the freshwater pearl mussel

The mussel's habitat was predicted to be stable over all time horizons, with maximum range shifts consistently below 3% of the modelled river network (Table 4). The future share of suitable habitat was predicted to be within 34.8%–39.0% of the simulated river network. Negligible changes in HSI were detected with the paired baseline versus scenario *t*-test (Table 4). Thus, the spatial arrangement of habitat patches potentially suitable for adults and juveniles is expected to not to change in the future (patches in Figure 3).

A total of 90 habitat patches were delineated (length range: 300–2,750 m; Figure 3), primarily located in the main stems of the river network. The total amount of habitat patches covers 19% of the simulated river network. Patch-averaged HSI ranges between 0.52 and 0.67.

3.3 | Impact of fine bed material deposits on mussel's habitat

FBMD risk is predicted to increase in the future for the whole network, with the highest increase for risk class 3 (Figure S15). Thus, the patch-specific ARI increases, leading to the exclusion of a higher number of patches in the future. In the baseline scenario, 93.3% of the habitat patches are not affected by FBMDs (corresponding to

TABLE 4 Freshwater pearl mussel available habitat and range shifts. All percentages are calculated as fractions of the total modelled spatial extent (n = 5,700 raster cells). Range expansions and contractions refer to the fraction of habitat that is respectively switched to suitable or rendered unsuitable with climate change

Scenario	Range expansion (%)	Range contraction (%)	Available habitat (%)	Baseline versus scenario t-test on HIS
Baseline	–	–	37.5	–
2060, RCP 4.5	1.9	2.7	36.7	Mean HSI change = −0.001; $t_{5663} = -3.36$, $p < 0.001$
2060, RCP 8.5	0.6	0.7	37.4	Mean HSI change = 0.0008; $t_{5663} = -2.34$, $p = 0.019$
2090, RCP 4.5	1.7	2.3	36.9	Mean HSI change = 0.0006; $t_{5663} = 4.48$, $p < 0.001$
2090, RCP 8.5	3.1	1.6	39.0	Mean HSI change = −0.009; $t_{5663} = 19.89$, $p < 0.001$

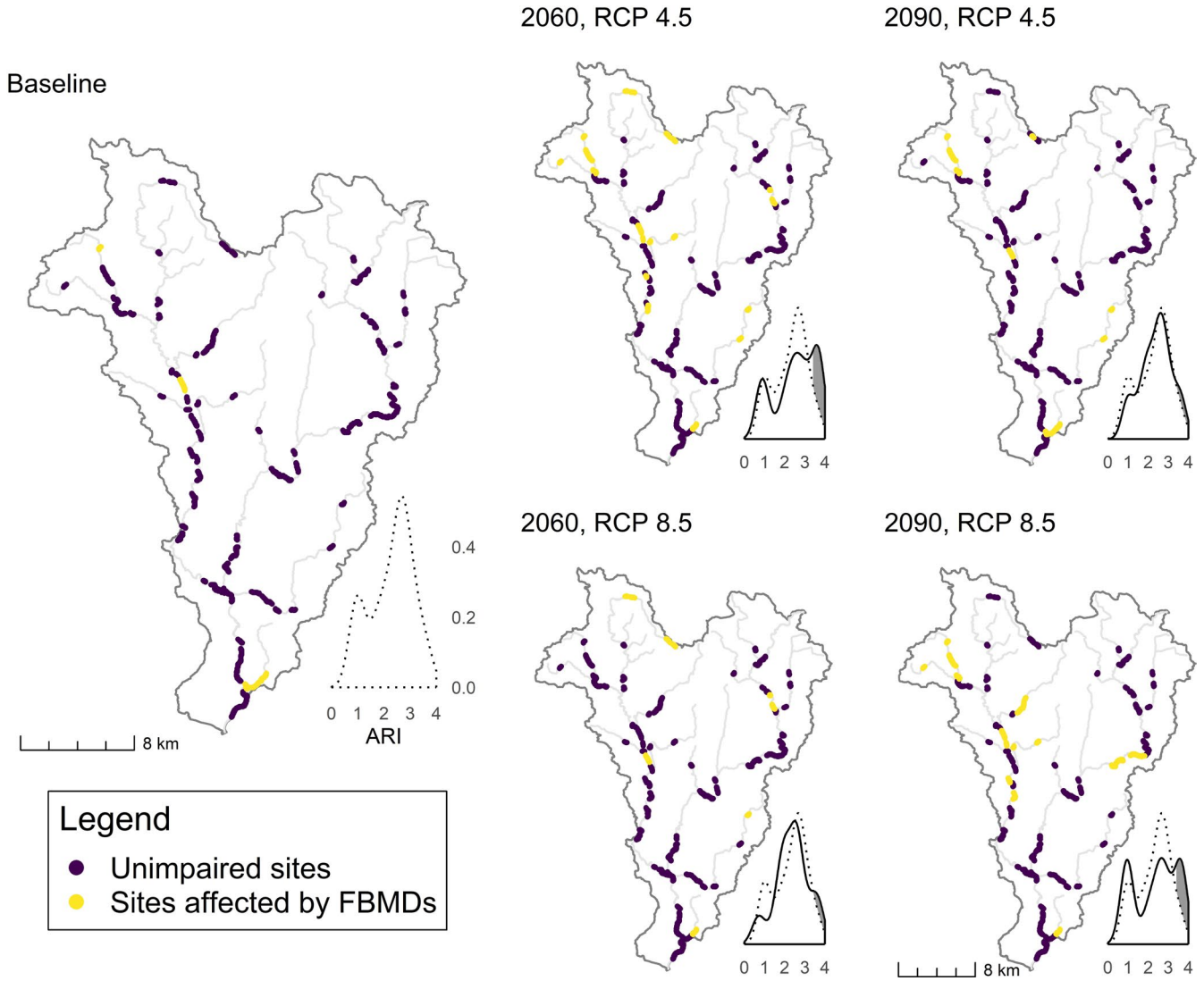

FIGURE 3 Spatial distribution of habitat patches that are impacted by FBMDs. The inserts aside of the maps show the ARI distribution for the baseline (dotted line) and for each scenario (full line). The shaded area between the two density plots represents the fraction of patches that get occupied by FBMDs

the 93.0% of the modelled river area). The impairment extent increases in 2060 for RCP 4.5 (73.3% of the patches and 80.3% of the area not affected, Figure 4) and in 2090 for RCP 8.5 (75.6% of the patches and 75.6% of the area). The position of impaired patches is mostly located in the headwaters in 2060 for RCP 4.5, and in the main stems in 2090 for RCP 8.5 (Figure 3).

3.4 | Impact of fine beds material deposits on mussel's dispersal potential

The reduction of available patches leads to a reduction in the structural connectivity, as indicated by the decrease in the $PCinter_{res}$ for all scenarios (Figure 5). For the 1,000-m dispersal distance, the baseline $PCinter_{res}$ is 84.9% (confidence interval (CI): 73.0%–93.8%). The lowest $PCinter_{res}$ occurs in 2060 for RCP 4.5 (60.6%, CI: 44.3%–75.6%) and in 2090 for RCP 8.5 (61.6%, CI: 39.6%–77.3%). Similar patterns were detected for both the longest and the shortest dispersal distances. The lowest $PCinter_{res}$ (49.5%; CI: 24.0%–73.5%) was detected for d = 200 m, 2060, RCP 4.5.

4 | DISCUSSION

4.1 | Projecting mechanistically the effects of climate change

The modelling cascade allows tracking the causal chain through which the pressure of climate change (i.e. future precipitation and air temperature patterns) affects the hydrological and hydraulic regimes and impacts FBMDs, habitat conditions and connectivity. The reduced precipitation in 2060 for RCP 4.5 causes a reduction of all discharge magnitudes based on daily streamflow (mean, high flow, low flow). The change in the precipitation patterns occurring in 2090 for RCP 8.5 in combination with increases in evapotranspiration and reduced contribution from snowmelt triggers the decrease in high flow discharge (Schneider et al., 2013), cascading in lower flow velocity and lower shear stresses during high flow. As suitable habitat patches are characterized by low (<25 Pa) shear stress during high flows, the prevailing natural substrate (cobbles, pebbles) is stable (Figure S1; Morales et al., 2006). Incipient motion of FBMDs occurs at 1–10 Pa, leading to instability when deposited over the mussel's habitat (Figure S1). Additionally, future increased air temperature and reduced water levels can increase water temperature and lower dissolved oxygen, both detrimental for the mussel (Bolotov et al., 2018; Santos et al., 2015).

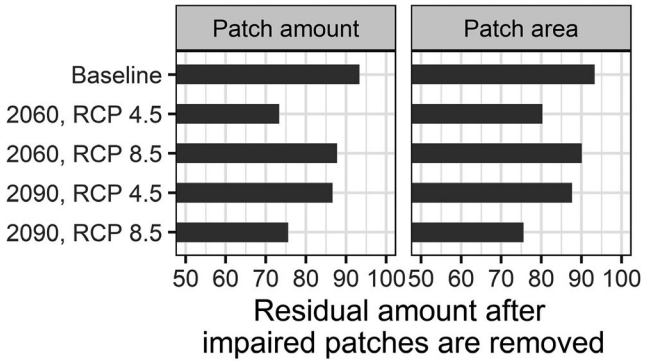

FIGURE 4 Relative drop in the number of habitat patch and the total patch areas when patches affected by FBMDs are removed. A value of 100 represents the theoretical value when no habitat patch is affected by FBMDs (unimpaired catchment)

The identified habitat patches that are likely to experience a future FBMD increase are located in subreaches with low transport capacity, decoupled from the upstream sediments supply (Baldan, Mehdi, et al., 2020). This explains the limited effect of the projected reduction in soil erosion on future FBMD distribution. However, the predicted reduction in soil erosion can stem out of models' and data limitations. Field measurements in the Aist catchment identified high-intensity, subdaily precipitation events as drivers for increased soil erosion in small subcatchments that, combined with a limited hydrological response in the main rivers, leads to FBMD accumulations (Hauer et al., 2015). Given the subdaily time-scales of such events, they could not be incorporated into the modelling framework (but they can be included with adequate data and resources). As the increased likelihood of such future extreme events was not considered, our results most likely underestimate the future spatial extent covered by FBMDs. Furthermore, extreme hydrological events can lead to adult detachment and die-offs (Sousa et al., 2012).

Despite the outlined limitations, we argue that ecohydrological modelling cascades support the development of semi-mechanistic ecohydrological relationships and ultimately improve their transferability to future scenarios (Yates et al., 2018). As shown here, implementing interlinked models is labour-intensive but can be considered a viable option for species with high conservation value.

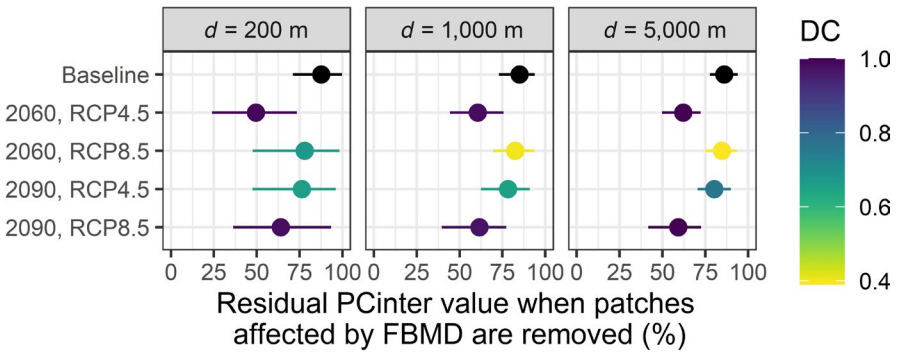

FIGURE 5 Residual PCinter calculated as patches affected by FBMDs are removed from the analysis for three different dispersal distances. A value of 100 represents the theoretical value when no habitat patch is affected by FBMDs (unimpaired catchment). DC was calculated for baseline versus scenario comparisons

4.2 | Planning freshwater pearl mussel conservation under climate change

Our results confirm how FBMDs are likely to expose the freshwater pearl mussel to an increased pressure under climate change. Mitigation and restoration actions are needed to avoid such increased habitat losses in the future. FBMDs can be targeted with sediment control measures in the catchment and in the riparian zone, such as sediment retention ponds, vegetated filter strips along the edges of agricultural fields and reintroduction of riparian vegetation (Baldan, Mehdi, et al., 2020). However, as sites with high FBMD risk are transport limited, such measures would not be completely effective if the capacity of the stream to mobilize the deposited material is not activated (Auerswald & Geist, 2018; Denic & Geist, 2015). For this purpose, cross-sectional modifications can be implemented to increase the transport capacity of the stream (Hauer, 2015). Ponds that store water and trap sediments during intense precipitation events might reduce the stream transport capacity by lowering high flows, increasing FBMD accumulation risk (Baldan, Mehdi, et al., 2020).

Based on the model's results, FBMD mitigation measures could be spatially allocated in the Aist catchment. For RCP 4.5, measures can be implemented in the north-western part of the Aist catchment, as habitat patches are persistently occupied in both time horizons. For RCP 8.5, the priority should be the contiguous sequence of patches in the mid-section of the eastern tributary connecting the north-eastern part of the catchment.

Common conservation practices for freshwater pearl mussels include restoring the local aquatic habitat to meet the mussel's hydraulic requirements, catchment-scale actions to improve water quality and artificial breeding and reintroduction (Geist, 2010). With this study, we argue that controlling FBMDs is also relevant, given the importance of this pressure for many freshwater pearl mussel catchments in Europe and the projected increase with decreasing flows in the future (Knott et al., 2019; Schneider et al., 2013).

4.3 | Climate change affects habitat connectivity

Conservation plans that incorporate organism dispersal and habitat connectivity are more likely to be effective in the future (Bush et al., 2014; Bush & Hoskins, 2017). Dispersal is relevant for freshwater mussels as it is the only mechanism to achieve the colonization of unoccupied suitable patches, while poor dispersal results in fragmented populations and local extinctions (Inoue & Berg, 2017; Vaughn, 2012), threatening the survival of metapopulations.

Habitat patches affected by FBMDs can still host overaged populations lacking the youngest age classes (Österling et al., 2010), but are unlikely to be colonized by juveniles. When FBMDs are persistent over a long time, even the long life span of the mussel cannot buffer against these disturbances (Österling et al., 2010). When patches are rendered unsuitable, the average inter-patch travel distance increases and the likelihood of successful dispersal decreases. The connectivity assessment suffers from some uncertainties. First, the future habitat of the brown trout could shift towards headwaters due to increasing water temperatures (Wenger et al., 2011). Second, the detected change in peak discharge timing for RCP 8.5 could impair the brown trout recruitment (Hauer et al., 2013). Finally, longitudinal barriers further limit the dispersal range (Buddendorf et al., 2019) but were not considered in our analysis. Thus, our results likely underestimate the future drops in dispersal likelihood.

Despite the simplified approach applied, we argue that the detected future trends in connectivity should be accounted for in a conservation plan that aims at sustaining functional and resilient metapopulations. A prioritization of habitat patches based on the relative contribution to the overall connectivity (Saura & Rubio, 2010) can support targeting conservation efforts (e.g. habitat improvement) in those sites that are more important to support effective dispersal.

5 | CONCLUSIONS

In this study, we projected the impacts of climate change on the freshwater pearl mussel, an organism with a complex life cycle relying on a host fish for dispersal. The use of a semi-mechanistic ecohydrological modelling cascade could significantly support the understanding of the system. We show how a future increase in FBMDs cascades into a reduction of the available mussel's habitat and a decrease in the likelihood of successful colonization. A conservation plan that aims to support future healthy mussel's metapopulations should focus on mitigating FBMDs, prioritizing those subreaches that offer the highest potential for preserving the connectivity among suitable habitats. Given the widespread distribution of the freshwater pearl mussel in Europe, its conservation status and vulnerability, this (or a similar) modelling framework could be implemented in other basins to link hydrological pressures and ecological responses, to support the development of effective conservation plans.

ACKNOWLEDGEMENTS

DB received support from the EU-INTERREG project FRAMWAT (grant number CE983), the Niederösterreiche Forschungs- und Bildungsgesellschaft scholarship (NFB grant number SC17-002), the Docstoral School 'Human River Systems in the 21st Century (HR21)' of the University of Natural Resources and Life Sciences (BOKU), Vienna, and the CEEPUS network EcoManAqua CIII-AT-1101-03-1819. J.K. and S.C.J. acknowledge funding through the 'GLANCE' project (Global change effects on river ecosystems; 01LN1320A) supported by the German Federal Ministry of Education and Research (BMBF) and support through the Deutsche Forschungsgemeinschaft (DFG, German Research Foundation) for CRC RESIST (1439/1, Project-Nr. 426547801). S.C.J. acknowledges funding through the Leibniz Competition for the project 'Freshwater Megafauna Futures'. The authors are also thankful to Laura Emily Coulson for proofreading the manuscript, Libor Zavorka for the useful information on the brown trout swimming capacity, Matthias

Pucher for the suggestions on the plots, Ignacy Kardel, and Robert Michałowski for the IT support.

AUTHORS' CONTRIBUTIONS

D.B. and T.H. conceived the ideas and designed the methodology; D.B., C.H., J.K. and S.C.J. collected the data; D.B. and J.K. analysed the data; D.B. led the writing of the manuscript. All the authors contributed critically to the drafts and gave final approval for publication.

DATA AVAILABILITY STATEMENT

Data available via the Zenodo Digital Repository https://doi.org/10.5281/zenodo.4911882 (Baldan et al., 2021).

ORCID

Damiano Baldan https://orcid.org/0000-0001-9237-4883
Thomas Hein https://orcid.org/0000-0002-7767-4607

REFERENCES

Allouche, O., Tsoar, A., & Kadmon, R. (2006). Assessing the accuracy of species distribution models: Prevalence, kappa and the true skill statistic (TSS). *Journal of Applied Ecology*, *43*(6), 1223–1232. https://doi.org/10.1111/j.1365-2664.2006.01214.x

Auerswald, K., & Geist, J. (2018). Extent and causes of siltation in a headwater stream bed: Catchment soil erosion is less important than internal stream processes. *Land Degradation and Development*, *29*(3), 737–748. https://doi.org/10.1002/ldr.2779

Baldan, D., Kiesel, J., Hauer, C., Jaehnig, S. C., & Hein, T. (2021). Data from: Increased sediment deposition triggered by climate change impacts freshwater pearl mussel habitats and metapopulations. *Zenodo Digital Repository*, https://doi.org/10.5281/zenodo.4911882

Baldan, D., Mehdi, B., Feldbacher, E., Piniewski, M., Hauer, C., & Hein, T. (2020). Assessing multi-scale effects of natural water retention measures on in-stream fine bed material deposits with a modeling cascade. *Journal of Hydrology*, *594*, 125702. https://doi.org/10.1016/j.jhydrol.2020.125702

Baldan, D., Piniewski, M., Funk, A., Gumpinger, C., Flödl, P., Höfer, S., Hauer, C., & Hein, T. (2020). A multi-scale, integrative modeling framework for setting conservation priorities at the catchment scale for the freshwater pearl mussel *Margaritifera margaritifera*. *Science of the Total Environment*, *718*, 137369. https://doi.org/10.1016/j.scitotenv.2020.137369

Barbet-Massin, M., Jiguet, F., Albert, C. H., & Thuiller, W. (2012). Selecting pseudo-absences for species distribution models: How, where and how many? *Methods in Ecology and Evolution*, *3*(2), 327–338. https://doi.org/10.1111/j.2041-210X.2011.00172.x

Bolla Pittaluga, M., Luchi, R., & Seminara, G. (2014). On the equilibrium profile of river beds. *Journal of Geophysical Research: Earth Surface*, *119*(2), 317–332. https://doi.org/10.1002/2013JF002806

Bolotov, I. N., Makhrov, A. A., Gofarov, M. Y., Aksenova, O. V., Aspholm, P. E., Bespalaya, Y. V., Kabakov, M. B., Kolosova, Y. S., Kondakov, A. V., Ofenböck, T., Ostrovsky, A. N., Popov, I. Y., von Proschwitz, T., Rudzīte, M., Rudzītis, M., Sokolova, S. E., Valovirta, I., Vikhrev, I. V., Vinarski, M. V., & Zotin, A. A. (2018). Climate warming as a possible trigger of keystone mussel population decline in oligotrophic rivers at the continental scale. *Scientific Reports*, *8*(1), 1–9. https://doi.org/10.1038/s41598-017-18873-y

Boon, P. J., Cooksley, S. L., Geist, J., Killeen, I. J., Moorkens, E. A., & Sime, I. (2019). Developing a standard approach for monitoring freshwater pearl mussel (*Margaritifera margaritifera*) populations in European rivers. *Aquatic Conservation: Marine and Freshwater Ecosystems*, *29*(8), 1365–1379. https://doi.org/10.1002/aqc.3016

Buddendorf, W. B., Jackson, F. L., Malcolm, I. A., Millidine, K. J., Geris, J., Wilkinson, M. E., & Soulsby, C. (2019). Integration of juvenile habitat quality and river connectivity models to understand and prioritise the management of barriers for Atlantic salmon populations across spatial scales. *Science of the Total Environment*, *655*, 557–566. https://doi.org/10.1016/j.scitotenv.2018.11.263

Bush, A., Hermoso, V., Linke, S., Nipperess, D., Turak, E., & Hughes, L. (2014). Freshwater conservation planning under climate change: Demonstrating proactive approaches for Australian Odonata. *Journal of Applied Ecology*, *51*(5), 1273–1281. https://doi.org/10.1111/1365-2664.12295

Bush, A., & Hoskins, A. J. (2017). Does dispersal capacity matter for freshwater biodiversity under climate change? *Freshwater Biology*, *62*(2), 382–396. https://doi.org/10.1111/fwb.12874

Denic, M., & Geist, J. (2015). Linking stream sediment deposition and aquatic habitat quality in pearl mussel streams: Implications for conservation. *River Research and Applications*, *31*(8), 943–952. https://doi.org/10.1002/rra.2794

Fuller, M. R., Doyle, M. W., & Strayer, D. L. (2015). Causes and consequences of habitat fragmentation in river networks. *Annals of the New York Academy of Sciences*, *1355*(1), 31–51.

Geist, J. (2010). Strategies for the conservation of endangered freshwater pearl mussels (*Margaritifera margaritifera* L.): A synthesis of conservation genetics and ecology. *Hydrobiologia*, *644*(1), 69–88. https://doi.org/10.1007/s10750-010-0190-2

Geist, J., & Auerswald, K. (2007). Physicochemical stream bed characteristics and recruitment of the freshwater pearl mussel (*Margaritifera margaritifera*). *Freshwater Biology*, *52*(12), 2299–2316. https://doi.org/10.1111/j.1365-2427.2007.01812.x

Gupta, H. V., Kling, H., Yilmaz, K. K., & Martinez, G. F. (2009). Decomposition of the mean squared error and NSE performance criteria: Implications for improving hydrological modelling. *Journal of Hydrology*, *377*(1–2), 80–91. https://doi.org/10.1016/j.jhydrol.2009.08.003

Hagemann, S., Chen, C., Clark, D. B., Folwell, S., Gosling, S. N., Haddeland, I., Hanasaki, N., Heinke, J., Ludwig, F., Voss, F., & Wiltshire, A. J. (2013). Climate change impact on available water resources obtained using multiple global climate and hydrology models. *Earth System Dynamics*, *4*(1), 129–144. https://doi.org/10.5194/esd-4-129-2013

Hauer, C. (2015). Review of hydro-morphological management criteria on a river basin scale for preservation and restoration of freshwater pearl mussel habitats. *Limnologica*, *50*, 40–53. https://doi.org/10.1016/j.limno.2014.11.002

Hauer, C., Höfler, S., Dossi, F., Flödl, P., Graf, W., Gstöttenmayr, D., & Habersack, H. (2015). *Feststoffmanagement im mühlviertel und im Bayerischen Wald*. Endbericht. 391.

Hauer, C., Unfer, G., Holzmann, H., Schmutz, S., & Habersack, H. (2013). The impact of discharge change on physical instream habitats and its response to river morphology. *Climatic Change*, *116*(3–4), 827–850. https://doi.org/10.1007/s10584-012-0507-4

HDLO. (2017). *Precipitation, temperature for 13 weather stations; discharge for 5 gauging stations*. Hydrographischer Dienst des Landes Oberösterreich.

Hoess, R., & Geist, J. (2020). Spatiotemporal variation of streambed quality and fine sediment deposition in five freshwater pearl mussel streams, in relation to extreme drought, strong rain and snow melt. *Limnologica*, *85*, 125833. https://doi.org/10.1016/j.limno.2020.125833

Inoue, K., & Berg, D. J. (2017). Predicting the effects of climate change on population connectivity and genetic diversity of an imperiled freshwater mussel, *Cumberlandia monodonta* (Bivalvia: Margaritiferidae), in riverine systems. *Global Change Biology*, *23*(1), 94–107. https://doi.org/10.1111/gcb.13369

Inoue, K., Stoeckl, K., & Geist, J. (2017). Joint species models reveal the effects of environment on community assemblage of freshwater

mussels and fishes in European rivers. *Diversity and Distributions*, *23*(3), 284–296. https://doi.org/10.1111/ddi.12520

IUCN. (2021). *The IUCN Red List of threatened species. Version 2021-1*. Retrieved from https://www.iucnredlist.org. Downloaded on 26th April 2021.

Jähnig, S. C., Kuemmerlen, M., Kiesel, J., Domisch, S., Cai, Q., Schmalz, B., & Fohrer, N. (2012). Modelling of riverine ecosystems by integrating models: Conceptual approach, a case study and research agenda. *Journal of Biogeography*, *39*(12), 2253–2263. https://doi.org/10.1111/jbi.12009

Kail, J., Guse, B., Radinger, J., Schröder, M., Kiesel, J., Kleinhans, M., Schuurman, F., Fohrer, N., Hering, D., & Wolter, C. (2015). A modelling framework to assess the effect of pressures on river abiotic habitat conditions and biota. *PLoS ONE*, *10*(6), 1–21. https://doi.org/10.1371/journal.pone.0130228

Kiesel, J., Gericke, A., Rathjens, H., Wetzig, A., Kakouei, K., Jähnig, S. C., & Fohrer, N. (2019). Climate change impacts on ecologically relevant hydrological indicators in three catchments in three European ecoregions. *Ecological Engineering*, *127*(December 2018), 404–416. https://doi.org/10.1016/j.ecoleng.2018.12.019

Kiesel, J., Stanzel, P., Kling, H., Fohrer, N., Jähnig, S. C., & Pechlivanidis, I. (2020). Streamflow-based evaluation of climate model subselection methods. *Climatic Change*, *163*(3), 1267–1285. https://doi.org/10.1007/s10584-020-02854-8

Knott, J., Mueller, M., Pander, J., & Geist, J. (2019). Effectiveness of catchment erosion protection measures and scale-dependent response of stream biota. *Hydrobiologia*, *830*(1), 77–92. https://doi.org/10.1007/s10750-018-3856-9

Modesto, V., Ilarri, M., Souza, A. T., Lopes-Lima, M., Douda, K., Clavero, M., & Sousa, R. (2018). Fish and mussels: Importance of fish for freshwater mussel conservation. *Fish and Fisheries*, *19*(2), 244–259. https://doi.org/10.1111/faf.12252

Morales, Y., Weber, L. J., Mynett, A. E., & Newton, T. J. (2006). Effects of substrate and hydrodynamic conditions on the formation of mussel beds in a large river. *Journal of the North American Benthological Society*, *25*(3), 664–676. https://doi.org/10.1899/0887-3593(2006)25[664:EOSAHC]2.0.CO;2

Olden, J. D., & Poff, N. L. (2003). Redundancy and the choice of hydrologic indices for characterizing streamflow regimes. *River Research and Applications*, *19*(2), 101–121. https://doi.org/10.1002/rra.700

Österling, M. E., Arvidsson, B. L., & Greenberg, L. A. (2010). Habitat degradation and the decline of the threatened mussel *Margaritifera margaritifera*: Influence of turbidity and sedimentation on the mussel and its host. *Journal of Applied Ecology*, *47*(4), 759–768. https://doi.org/10.1111/j.1365-2664.2010.01827.x

Rathjens, H., Bieger, K., Srinivasan, R., Chaubey, I., & Arnold, J. G. (2016). *CMhyd User Manual: Documentation for preparing simulated climate change data for hydrologic impact studies*.

Santos, R., Sanches Fernandes, L. F., Varandas, S., Pereira, M. G., Sousa, R., Teixeira, A., Lopes-Lima, M., Cortes, R., & Pacheco, F. (2015). Impacts of climate change and land-use scenarios on *Margaritifera margaritifera*, an environmental indicator and endangered species. *Science of the Total Environment*, *511*, 477–488. https://doi.org/10.1016/j.scitotenv.2014.12.090

Saura, S., & Rubio, L. (2010). A common currency for the different ways in which patches and links can contribute to habitat availability and connectivity in the landscape. *Ecography*, *33*(3), 523–537. https://doi.org/10.1111/j.1600-0587.2009.05760.x

Schneider, C., Laizé, C. L. R., Acreman, M. C., & Flörke, M. (2013). How will climate change modify river flow regimes in Europe? *Hydrology and Earth System Sciences*, *17*(1), 325–339. https://doi.org/10.5194/hess-17-325-2013

Sousa, R., Amorim, Â., Froufe, E., Varandas, S., Teixeira, A., & Lopes-Lima, M. (2015). Conservation status of the freshwater pearl mussel *Margaritifera margaritifera* in Portugal. *Limnologica*, *50*, 4–10. https://doi.org/10.1016/j.limno.2014.07.004

Sousa, R., Ferreira, A., Carvalho, F., Lopes-Lima, M., Varandas, S., & Teixeira, A. (2018). Die-offs of the endangered pearl mussel *Margaritifera margaritifera* during an extreme drought. *Aquatic Conservation: Marine and Freshwater Ecosystems*, *28*(5). https://doi.org/10.1002/aqc.2945

Sousa, R., Ferreira, A., Carvalho, F., Lopes-Lima, M., Varandas, S., Teixeira, A., & Gallardo, B. (2020). Small hydropower plants as a threat to the endangered pearl mussel *Margaritifera margaritifera*. *Science of the Total Environment*, *719*, 137361. https://doi.org/10.1016/j.scitotenv.2020.137361

Sousa, R., Varandas, S., Cortes, R., Teixeira, A., Lopes-Lima, M., MacHado, J., & Guilhermino, L. (2012). Massive die-offs of freshwater bivalves as resource pulses. *Annales de Limnologie*, *48*(1), 105–112. https://doi.org/10.1051/limn/2012003

Switanek, M. B., Troch, P. A., Castro, C. L., Leuprecht, A., Chang, H.-I., Mukherjee, R., & Demaria, E. (2017). Scaled distribution mapping: A bias correction method that preserves raw climate model projected changes. *Hydrology and Earth System Sciences*, *21*(6), 2649–2666.

Thuiller, W., Lafourcade, B., Engler, R., & Araújo, M. B. (2009). BIOMOD–a platform for ensemble forecasting of species distributions. *Ecography*, *32*(3), 369–373. https://doi.org/10.1111/j.1600-0587.2008.05742.x

Varandas, S., Lopes-Lima, M., Teixeira, A., Hinzmann, M., Reis, J., Cortes, R., Machado, J., & Sousa, R. (2013). Ecology of southern European pearl mussels (*Margaritifera margaritifera*): First record of two new populations on the rivers Terva and Beça (Portugal). *Aquatic Conservation: Marine and Freshwater Ecosystems*, *23*(3), 374–389. https://doi.org/10.1002/aqc.2321

Vaughn, C. C. (2012). Life history traits and abundance can predict local colonisation and extinction rates of freshwater mussels. *Freshwater Biology*, *57*(5), 982–992. https://doi.org/10.1111/j.1365-2427.2012.02759.x

Ward, M., Saura, S., Williams, B., Ramírez-Delgado, J. P., Arafeh-Dalmau, N., Allan, J. R., Venter, O., Dubois, G., & Watson, J. E. M. (2020). Just ten percent of the global terrestrial protected area network is structurally connected via intact land. *Nature Communications*, *11*(1), 1–10. https://doi.org/10.1038/s41467-020-18457-x

Wenger, S. J., Isaak, D. J., Luce, C. H., Neville, H. M., Fausch, K. D., Dunham, J. B., Dauwalter, D. C., Young, M. K., Elsner, M. M., Rieman, B. E., Hamlet, A. F., & Williams, J. E. (2011). Flow regime, temperature, and biotic interactions drive differential declines of trout species under climate change. *Proceedings of the National Academy of Sciences of the United States of America*, *108*(34), 14175–14180. https://doi.org/10.1073/pnas.1103097108

Yates, K. L., Bouchet, P. J., Caley, M. J., Mengersen, K., Randin, C. F., Parnell, S., Fielding, A. H., Bamford, A. J., Ban, S., Barbosa, A. M., Dormann, C. F., Elith, J., Embling, C. B., Ervin, G. N., Fisher, R., Gould, S., Graf, R. F., Gregr, E. J., Halpin, P. N., … Sequeira, A. M. M. (2018). Outstanding challenges in the transferability of ecological models. *Trends in Ecology and Evolution*, *33*(10), 790–802. https://doi.org/10.1016/j.tree.2018.08.001

Young, R. G., Hayes, J. W., Wilkinson, J., & Hay, J. (2010). Movement and mortality of adult brown trout in the Motupiko River, New Zealand: Effects of water temperature, flow, and flooding. *Transactions of the American Fisheries Society*, *139*(1), 137–146. https://doi.org/10.1577/t08-148.1

SUPPORTING INFORMATION

Additional supporting information may be found online in the Supporting Information section.

How to cite this article: Baldan, D., Kiesel, J., Hauer, C., Jähnig, S. C., & Hein, T. (2021). Increased sediment deposition triggered by climate change impacts freshwater pearl mussel habitats and metapopulations. *Journal of Applied Ecology*, 58, 1933–1944. https://doi.org/10.1111/1365-2664.13940